PERKIN 2

Fluorescent behaviour in host–guest interactions. Part 2.† Thermal and pH-dependent sensing properties of two geometric isomers of fluorescent amino-β-cyclodextrin derivatives

Hironori Nakashima,[a] Yasushi Takenaka,[a] Miwako Higashi[b] and Noboru Yoshida *[a]

[a] *Laboratory of Molecular Functional Chemistry, Division of Material Science, Graduate School of Environmental Earth Science, Hokkaido University, Sapporo 060-0810, Japan*
[b] *Center for Cooperative Research and Development, Ibaraki University, Hitachi 316-8511, Japan*

Received (in Cambridge, UK) 3rd July 2001, Accepted 15th August 2001
First published as an Advance Article on the web 16th October 2001

The fluorescent behaviour in aqueous solution of two types of amino-β-cyclodextrin (amino-β-CDx) isomers **1** and **2** bearing the naphthoamide group at the 1- and 2-position as a fluorescent-sensing unit was investigated using mainly fluorescence spectroscopy. The isomers **1** and **2** show both strong temperature- and pH-responsive photophysical properties in aqueous solution. The protonation of the amino groups of **1** and **2** in acidic media affects efficiently their fluorescence intensities. The equilibrium and thermodynamic quantities of the two-state equilibrium model for **1** and **2** have been determined spectrophotometrically. Solution NMR behaviour in a DMSO–D_2O mixed solvent confirms the stereospecific relationship between the appended naphthalene fluorophore and the hydrophobic cavity of CDx. Restricted and/or flexible motion of the naphthalene moiety of **1** and **2** about the bond between the amide group and the amino group at the C-6 carbon atom in the CDx ring is evident from the NMR studies. The potential application of **1** to anion sensing is also discussed.

Introduction

Molecular manufacturing is linked to many areas of science and technology.[1] In particular, research in molecular machinery requires a design perspective because it aims to describe workable systems such as the molecular shuttle.[2] Recent use of cyclodextrins as building blocks for the construction of supramolecular species[3,4] such as rotaxanes, dendrimers and lipophilic chiral sensors[5] in solution is emerging as a new contemporary field in CDx chemistry.

To date we have focussed our attention on the molecular recognition phenomena of several anionic azo compounds by α-cyclodextrin as these systems provide a suitable dynamic model for enzyme–substrate binding processes in aqueous solution.[6–14] Also, weak interactions such as electrostatic forces have been found to be effective in the selectivity and enhancement of binding properties in amino-β-cyclodextrin systems[15–19] such as **3**,[16] **4**,[16] **5**[18] and **6**.[18] In particular, for **5**, a one-dimensional supramolecular array with a helically extended polymeric structure has been found to form in the solid state by repetition of intermolecular inclusion.[18]

Fluorescent artificial cyclodextrins have received considerable attention in sensory,[20] biochemical[21] and photoelectronic[22] applications. The CDx cavity offering a binding site and a fluorophore acting as a signaling unit with a linkage group are indispensable for substrate specific-responsive functions. Isomers **1** and **2** are found to possess a wide range of features that render them attractive as potential sensors for temperature, pH and anions.

Here, we describe the novel temperature and pH sensing ability of **1** and **2**. The thermodynamic quantities of these processes and their potential application to anion sensing are also reported.

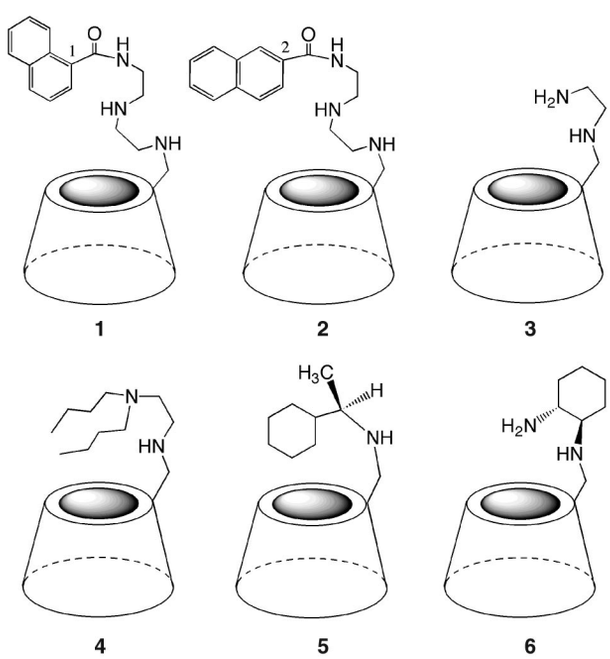

Experimental

Materials and synthesis

Analytical grade β-cyclodextrin (Wako Pure Chemical Ind. Ltd.) was used without further purification. Monotosylated β-CDxots at the O-6 position of the D-glucopyranosyl rings of β-CDx was synthesized by the reaction of *β*-CDx with toluene-*p*-sulfonyl chloride in pyridine at room temperature for 1.5 h (Scheme 1).[16] The *β*-CDxots thus obtained was dissolved in excess diethylenetriamine bis(2-aminoethyl)amine (Tokyo Kasei) and the solution was heated at 70 °C for 3 h with stirring.

† For Part 1 see ref. 16(*b*).

 DOI: 10.1039/b105875b

This journal is © The Royal Society of Chemistry 2001

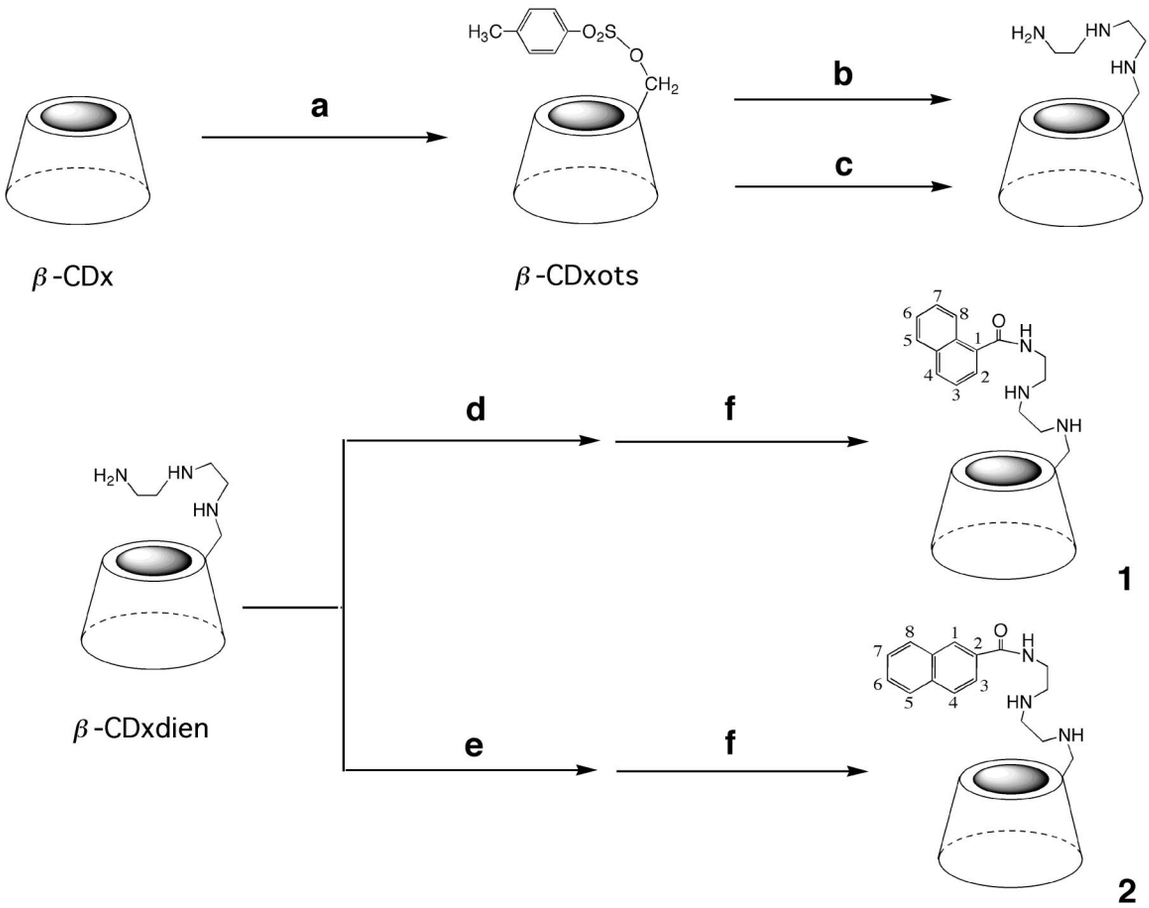

Scheme 1 Synthesis of **1** and **2**. *Reagents and conditions*: (a) *p*-TsCl, pyridine, room temp, 1.5h; (b) diethylenetriamine, 70 °C, 3 h; (c) cation exchange column chromatography; (d) 1-naphthoic acid, DCC, HOSu, DMF, 0 °C, 1 h, and then room temp; (e) 2-naphthoic acid, DCC, HOSu, DMF, 0 °C, 1 h, and then room temp; (f) cation-exchange column chromatography.

The reaction mixture was poured into a large amount of acetone and the resultant white precipitate was collected and dried *in vacuo*. Purification of mono[6-*N*-(5-amino-3-azapentyl)amino-6-deoxy]-β-cyclodextrin (β-CDxdien) as a precursor of the functionallized β-CDx derivatives was carried out by ion-exchange column chromatography through a cation-exchange resin (Toyopearl 650 M; 0.05 mol dm^{-3} NH_4HCO_3 aqueous solution as eluent). The purified β-CDxdien was then coupled with 1- and 2-naphthoic acid by the usual 1,3-dicyclohexylcarbodiimide (DCC) method and precipitation with acetone and cation-exchange chromatography gave **1** (yield, 48% based on β-CDxdien) and **2** (yield, 10% based on β-CDxdien), respectively (Scheme 1). The elemental analysis of **1** and **2** was satisfactory, although solvent water molecules were usually bound [Found for **1**: C, 46.23; H, 6.56; N, 2.71. Calc. for $C_{57}H_{87}N_3O_{35}\cdot 6H_2O$: C, 46.18; H, 6.73; N, 2.83%. Found for **2**: C, 47.87; H, 6.44; N, 3.18. Calc. for $C_{57}H_{87}N_3O_{35}\cdot 3H_2O$: C, 47.93; H, 6.56; N, 2.94%].

The ^{1}H NMR spectrum (external TMS, JEOL 400 MHz NMR spectrometer) of **1** shows characteristic peaks of the α-protons to the amino nitrogen at δ 2.6–3.0 in D_2O (pD 10): **1**, δ_H 2.6–3.0 (8H, N-CH_2), 3.3–3.6 (14H, 2-H and 4-H), 4.8–5.1 (7H, 1-H), and 3.5–4.0 (28H, 3-H, 5-H and 6-H) for the *β*-CDx ring protons and 7.5–8.3 (7H, aromatic protons). It is noteworthy that the C1-H protons of the D-glucopyranosyl moiety of the β-CDx ring of **1** shows seven different resonances. ^{13}C NMR (D_2O) for **1**: δ_C 39.83 (α-carbon to NHCO), 47.50–48.68 (methylene spacer and C-6 carrying NH), 60.33–60.60 (C-6 (CDx ring)), 70.85–73.80 (C-2, C-3, C-5), 81.36–84.09 (C-4), 102.22–102.56 (C-1), 125.27–133.88 (naphthalene moiety) and 172.84 (carbonyl). The ^{1}H NMR spectrum of **2** is also identical to that of **1** except for the spectral pattern in the aromatic region. ^{13}C NMR (D_2O) for **2**: δ_C 39.23 (α-carbon to NHCO), 45.99–50.10 (methylene spacer and C-6 carrying NH), 60.72–66.64 (C-6 (CDx ring)), 70.95–74.20 (C-2, C-3, C-5), 81.81–84.86 (C-4), 102.64–103.35 (C-1), 122.12–134.89 (naphthalene moiety) and 168.67 (carbonyl). Mass spectral data also coincide with the structural formula [MS(FAB, *m*-nitrobenzyl alcohol (*m*-NBA) as matrix) *m*/*z* 1374 (MH^+) for **1** and 1374 (MH^+), 1396 $(M + Na)^+$, and 1413 $(M + K)^+$ for **2**.

Measurement of physical quantities

Equilibrium constants (*K*) for the temperature-dependent process of **1** and **2** were determined by fluorescence spectroscopy using a Shimadzu RF-5000 recording fluorescence spectrometer. The pH values in solution were obtained using a Horiba pH meter B-112. Below pH 5.5, HCl–HEPES (*N*-(2-hydroxyethyl)piperazine-*N*′-ethanesulfonic acid) at low concentration (<0.01 mol dm^{-3}) was used and above this pH, HEPES and NaOH were used. The temperature of the solution was controlled by means of an external circulating water bath (Thomas Kagaku Co. Ltd., TRL-108H). Relative fluorescence intensities were measured at a constant wavelength around the emission maximum. The NMR spectra of **1** and **2** were obtained at various temperatures with a JEOL EX400 FTNMR spectrometer. The CD spectra were measured using a JASCO J-600C circular dichrometer. In order to obtain an adequate signal-to-noise ratio, we used a computer for multiple scanning and averaging. Each memory unit in the computer stored the CD signal for a spectral band of 0.2 nm.

Results and discussion

Temperature-responsive fluorescence spectra of 1 and 2

The effect of temperature on the fluorescence spectrum of **1** is

shown in Fig. 1. A progressive decrease in temperature results in quite an enhancement in emission intensity. Fig. 2 shows the fluorescence intensity (I_F) *vs.* temperature plot for **1** at the emission maximum wavelength (λ_{em}(max)), which has a hyperbola profile with an inflection point at *ca.* 35 °C. Fluorescent amino-*β*-cyclodextrin derivative **2** bearing an amide-linkage at the 2-position of the naphthalene ring also exhibits a similar I_F–T profile as shown in Fig. 2 and an inflection point at *ca.* 50 °C, but its fluorescent intensity is much greater than that of **1** even at the 3.0 nm bandwidth used for both emission and excitation.

In order to clarify the strong temperature-dependent fluorescence spectra of **1** and **2**, we measured their ^{1}H NMR spectra at various temperatures (30, 40 and 60 °C). Fig. 3 shows the temperature-dependent ^{1}H NMR spectra of the naphthalene and CDx ring moieties of **1**. The protons in the naphthalene moiety show a small shift. Although the anomeric protons (H-1) of the native β-CDx exhibit only one degenerated resonance, those of the derivative **1** showed six separated resonances. Mono modification at the C-6 position of β-CDx causes the seven D-glucopyranosyl rings to have a magnetically inequivalent environment.[23] Therefore, the slight change in the spectral pattern in Fig. 3 for the anomeric protons at the higher temperature suggest a subtle change in the motion of each D-glucopyranosyl ring of **1**. However, the relationship between the self-inclusion (inside–outside isomerisation equilibrium) of the naphthalene unit of **1** into the CDx cavity and the temperature-dependent fluorescence spectra for **1** is not clear.

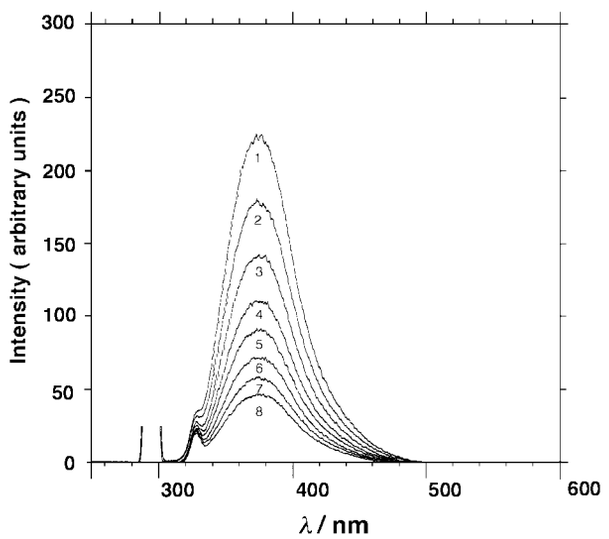

Fig. 1 Temperature-dependent fluorescence spectrum of **1**. [**1**] = 1.25 × 10^{-5} mol dm^{-3} and pH = 7.0. 10 (1), 20 (2), 30 (3), 40 (4), 50 (5), 60 (6), 70 (7) and 80 °C (8). The excitation (λ_{ex} = 295 nm) and emission bandwidth were both set at 5.0 nm.

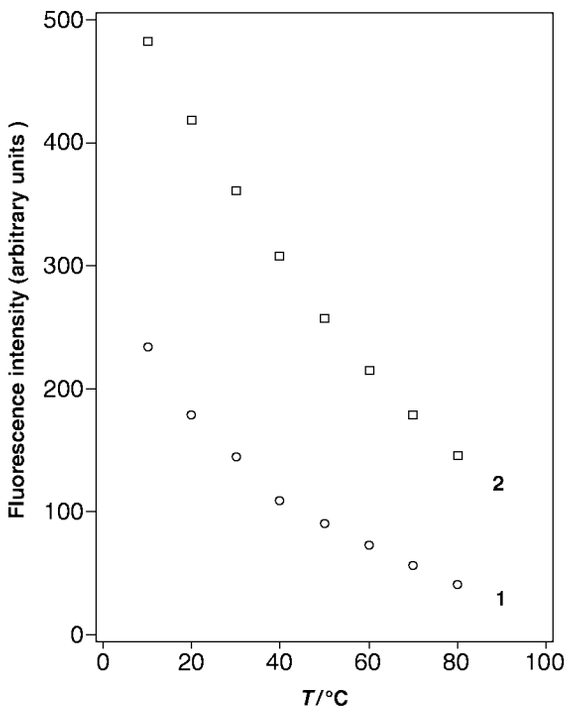

Fig. 2 Plots of fluorescence intensity at λ_{em}(max) *vs.* temperature (°C) for **1** and **2** at pH = 7. [**1**] = [**2**] = 1.25 × 10^{-5} mol dm^{-3}. The excitation and emission bandwidth for **2** were both set at 3.0 nm.

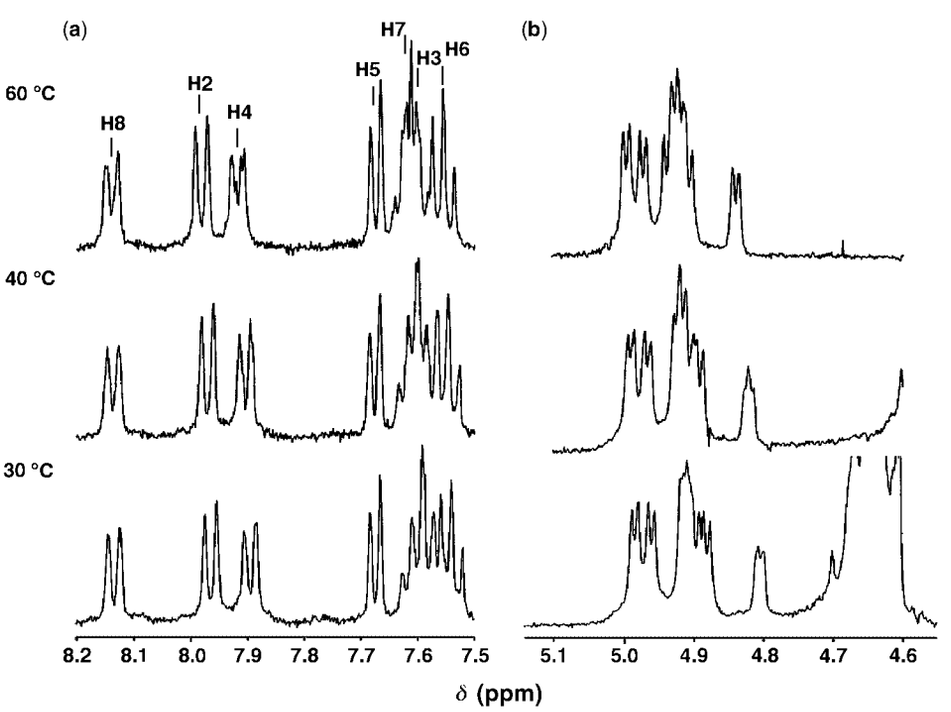

Fig. 3 ^{1}H NMR spectra of **1** at various temperatures in D_2O (ext. ref TMS). The aromatic region (a) and C1-H protons of the CDx ring (b) for **1** are shown. Numberings refer to those in Scheme 1. [**1**] = 7.28 × 10^{-3} mol dm^{-3}.

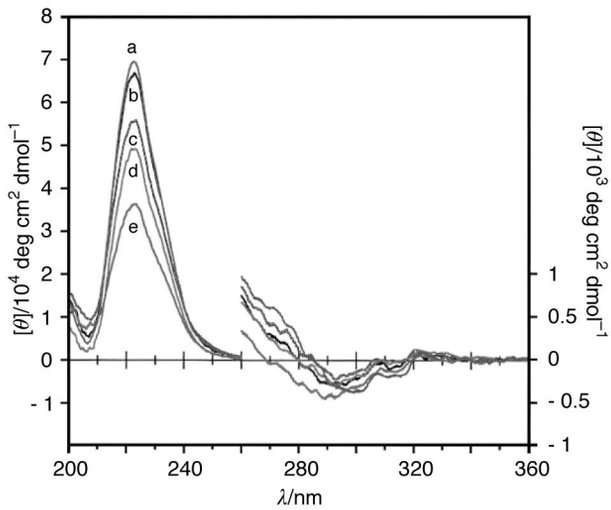

Fig. 4 Induced circular dichroism spectra of **1** at 10 (a), 25 (b), 40 (c), 60 (d) and 80 (e) °C. [**1**] = 1.25×10^{-5} mol dm^{-3}.

Fig. 4 shows the induced circular dichroism (ICD) spectrum of **1** at various temperatures. The ICD spectral change provides precise structural information such as the orientation of the chromophore in the CDx cavity.[24] If the polarization of the π–π* transition of the chromophore is almost parallel to the symmetry axis of CDx, the relatively strong positive ICD sign should be observed. The ICD sign at lower temperatures of **1** shows a larger positive value and its intensity gradually decreases upon increasing the temperature in solution. These ICD data suggest that the long-axis polarized π–π* transition of the chromophore is inclined against the CDx axis upon increasing the temperature, as shown in Scheme 2. This subtle

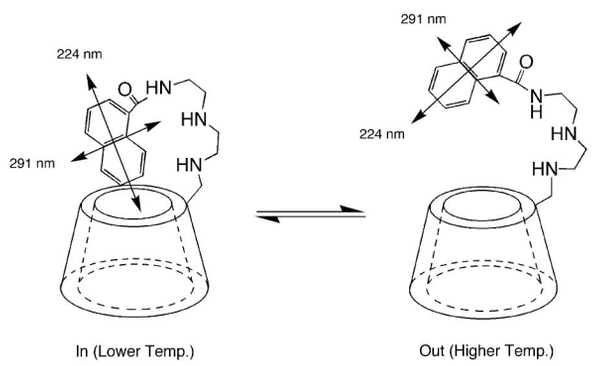

Scheme 2

conformational change may not be detected by the ^{1}H NMR spectrophotometric method. Furthermore, the concentration dependence (5.00×10^{-6}, 2.50×10^{-5}, 5.00×10^{-5}, 2.50×10^{-4} mol dm^{-3}) of the ICD of **1** was not observed.

Strongly temperature-dependent ^{1}H NMR spectrum of 2

By contrast, the ^{1}H NMR spectra of **2** were strongly temperature dependent as exemplified by its behaviour in D_2O (Fig. 5(a)). The most noticeable upfield shift upon decreasing the temperature was observed for the H-5, H-6, H-7 and H-8 naphthalene protons far from the amide linkage. Such an upfield shift in the NMR signal suggests that a regiospecific inclusion complexation between these protons and the CDx cavity may be involved.[16] The aromatic region of the ^{1}H NMR spectrum of **2** at 70 °C is almost similar to that of reference compound **7** in D_2O, indicating that the naphthalene fluorophore is situated outside the CDx cavity. Furthermore, the spectral pattern due to the anomeric H-1 protons of the CDx

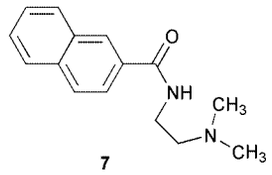

7

ring of **2** are also appreciably affected (Fig. 5(b)); each of the peaks shift downfield and converge to some extent.

Fig. 6 shows the plot of chemical shifts *vs.* temperature. The protons H-1, H-3, and H-4 at the periphery of the amide linkage show only a little shift, while the protons H-5, H-6, H-7 and H-8 show a large shift as mentioned above.

Stereospecific intramolecular and/or intermolecular inclusion takes place efficiently in **2** judging from the temperature dependence of the ^{1}H NMR spectrum. Perhaps, the difference in the linkage between the naphthalene unit and the amide group at the 1- or 2-position could determine whether such an inclusion process occurs. The suitable linkage position (2-isomer) for **2** led smoothly to the inclusion of the naphthalene unit into its CDx cavity. On the other hand, the amide group at the 1-position of **1** may result in a much shallower self-inclusion due to steric hindrance between the naphthalene moiety and the CDx cavity.

It is noteworthy that the intermolecular inclusion process shown in Scheme 3 may be formed in the concentrated solution

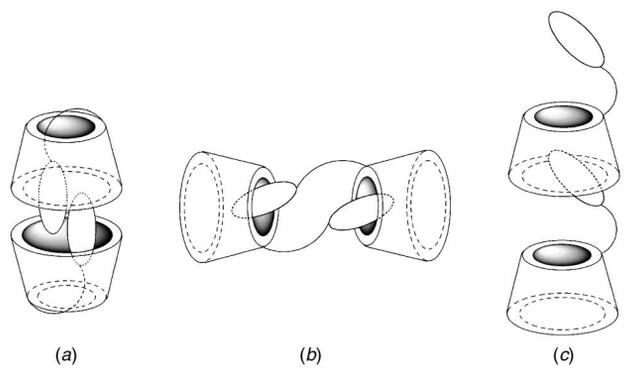

Scheme 3

(10^{-3} mol dm^{-3} under NMR conditions) and in the solid state. For example, type (c) complex has been found in the case of host **5** by X-ray crystallographic analysis.[18] Takahashi and Hattori also suggested this type of complex to occur in monosubstituted cyclodextrins based on their ^{1}H NMR analysis.[25] Furthermore, the existence of type (a)[26] and type (b)[27] has been also pointed out by some authors. Since the ^{1}H NMR of **2** is found to be concentration-dependent, the strongly temperature-dependent ^{1}H NMR spectrum of **2** shown in Fig. 5 is due to one of the intermolecular inclusion processes shown in Scheme 3. On the other hand, the ^{1}H NMR of **1** is almost concentration-independent. Furthermore, self-inclusion of the naphthalene probe of **2** may occur in dilute aqueous solution (10^{-5} mol dm^{-3}) judging by its smaller ICD spectral change at various temperatures.

Energetic preferences for the inclusion process for 1 and 2

The temperature-dependent fluorescence change could be analysed thermodynamically by a two-state equilibrium model.[28] The equilibrium constant K for the equilibrium between **1** and **2** in eqn. (1) can be expressed by eqn. (2), where $I_{f,\ lower\ temp.}$, $I_{f,\ higher\ temp.}$ and $I_{f,\ obs}$ denote the fluorescence intensity at λ_{em} for the lower-temperature and higher-temperature species and the observed experimental fluorescence intensity in Fig. 1, respectively. The temperature dependence of the equilibrium constant K is given by eqn. (3), where R and T are the

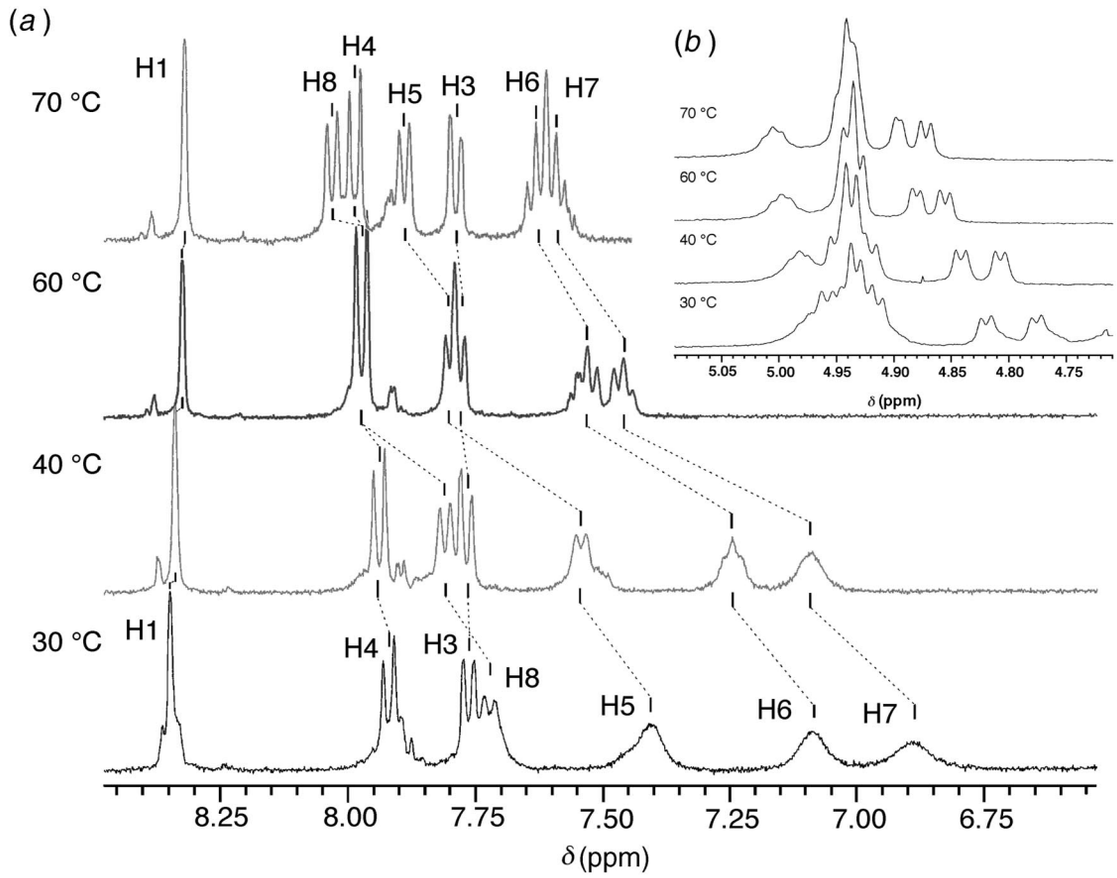

Fig. 5 ^{1}H NMR spectra of **2** at various temperatures in D_2O (ext. ref. TMS). Aromatic region (a) and C1-H protons of CDx ring (b) for **2** are shown. [**1**] = 7.28 × 10^{-3} mol dm^{-3}.

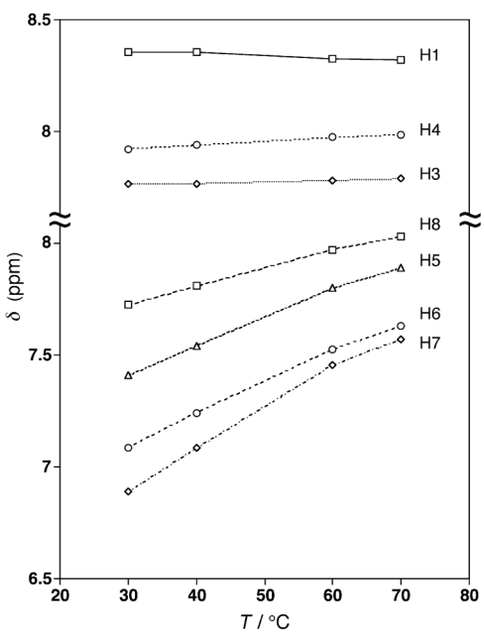

Fig. 6 Plots of the chemical shift [δ(ppm)] of appended naphthalene protons for **2** *vs.* temperature in aqueous solution.

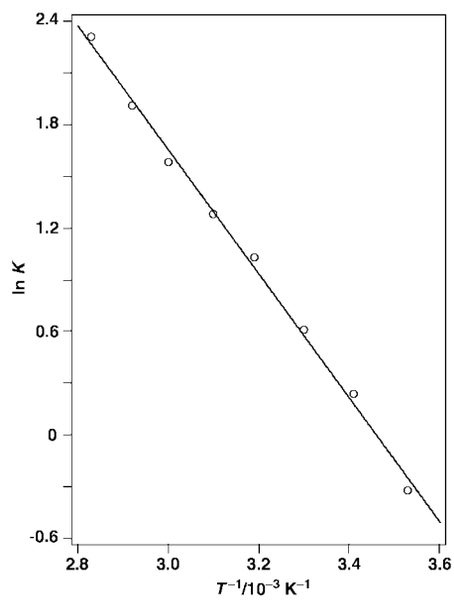

Fig. 7 Plot of ln K *vs.* T^{-1} for the inside–outside isomerisation of the appended naphthalene of **1**.

gas constant and absolute temperature, respectively. The least-squares fit for eqn. (3) has been carried out using the postulated values of $I_{\text{f, lower temp.}}$ and $I_{\text{f, higher temp}}$ until a good linear relationship in the ln K *vs.* T^{-1} plot could be obtained. An optimised linear plot of ln K for **1** against T^{-1} could be obtained as shown in Fig. 7 on the assumption that $I_{\text{f, lower temp}}$ and $I_{\text{f, higher temp}}$ are equal to 400 at −10 °C and 5 at 100 °C, respectively.

$$\mathbf{1}(\mathbf{2})_{\text{lower temp.}} \overset{K}{\rightleftharpoons} \mathbf{1}(\mathbf{2})_{\text{higher temp.}} \quad (1)$$

$$K = \frac{[\mathbf{1}(\mathbf{2})_{\text{higher temp.}}]}{[\mathbf{1}(\mathbf{2})_{\text{lower temp.}}]} = \frac{(I_{\text{f, lower temp.}} - I_{\text{f, obs}})}{(I_{\text{f, obs.}} - I_{\text{f, higher temp.}})} \quad (2)$$

$$\ln K = \ln \frac{(I_{\text{f, lower temp.}} - I_{\text{f, obs}})}{(I_{\text{f, obs.}} - I_{\text{f, higher temp.}})} = \frac{\Delta S^{\circ}}{R} - \frac{\Delta H^{\circ}}{RT} \quad (3)$$

The values of ΔH° and ΔS° were calculated from the slope and intercept through the van't Hoff plot in Fig. 7. A series of similar procedures were also carried out for derivative **2**.

Table 1 Thermodynamic parameters for the inside–outside isomerization of **1** and **2** at 20 °C in aqueous solution

	K (20 °C)	$\Delta H°$/kcal mol^{-1}	$\Delta S°$/cal K^{-1} mol^{-1}	$\Delta G°$/kcal mol^{-1}
1	1.27	7.13	24.7	−0.14
2	0.92	5.48	18.5	0.06

Table 2 Change in the chemical shift (δ (ppm)) of the naphthalene protons of **1** in the absence and presence of $NaClO_4$ at 30 and 70 °C in D_2O

	H-2	H-3	H-4	H-5	H-6	H-7	H-8
δ_a [a]	7.966	7.571	7.896	7.676	7.541	7.610	8.136
δ_b [b]	7.980	7.580	7.922	7.663	7.527	7.598	8.036
$\Delta\delta = \delta_b - \delta_a$	0.014	0.009	0.026	0.013	−0.014	−0.012	−0.050
δ_c [c]	7.996	7.602	7.940	7.669	7.548	7.621	8.130
$\Delta\delta = \delta_c - \delta_b$	0.016	0.022	0.018	0.006	0.021	0.023	0.017

[a] At 30 °C and [$NaClO_4$] = 0 mol dm^{-3}. [b] At 30 °C and [$NaClO_4$] = 2 mol dm^{-3}. [c] At 70 °C and [$NaClO_4$] = 2 mol dm^{-3}.

Thermodynamic parameters for the two-state equilibria of **1** and **2** are given in Table 1.

In general, cyclodextrin inclusion for various guests is enthalpically driven ($\Delta H°_{incl} < 0$) and the standard entropy change is either negative or positive.[6,9,12,28] Therefore, the positive $\Delta H°$ values ($-\Delta H°_{incl}$) in our case indicate that the exclusion of the naphthalene unit from the CDx cavity is endothermic for both **1** and **2**. The more positive value of $\Delta H°$ for **1** suggests restrictive motional freedom of the naphthalene ring when the amide linkage is at the 1-position. In all cases the inclusion is enthalpically favoured ($\Delta H°_{incl} < 0$) but entropically unfavoured ($\Delta S°_{incl} < 0$). It is noteworthy that the comparative contribution of $\Delta S°$ to the Gibbs energy term $\Delta G°$ shows a positive value which results from two different contributions:[10] the changes in (i) randomness and (ii) solvation which are associated with the two-state inclusion model.

Effect of anions

Upon addition of several inorganic salts, the considerable fluorescence quenching and/or large enhancement in intensity were observed only in the **1**–anion system. Addition of Cl^- and SO_4^{2-} anions has little effect on the fluorescence intensity (I_f) of **1**. On the other hand, Br^-, I^-, and SCN^- quench the fluorescence intensity appreciably. Interestingly, the addition of a bulky hydrophobic anion such as ClO_4^- and PF_6^- results in a large enhancement in I_f. This unexpected enhancement in I_f is not observed in **2**. It is well known that ClO_4^- and PF_6^- can be included into the β-CDx cavity,[30] so perhaps, derivative **1** would have enough space in its cavity to accommodate such anions. Table 2 shows the change in the chemical shift of the naphthalene protons of **1** in the presence of $NaClO_4$. The upfield shift ($\Delta\delta = \delta_b - \delta_a$) of H-6, H-7 and H-8 indicates the shallower induced-inclusion into the β-CDx cavity upon addition of the anions (Scheme 4). This upfield shift is reduced ($\Delta\delta = \delta_c - \delta_b >$ 0) upon increasing the temperature to 70 °C. Fig. 8 shows the temperature dependence of I_f for **1** on the concentration of $NaClO_4$. At lower temperatures, the magnitude of the fluorescence enhancement in the presence of $NaClO_4$ is particularly large. The effect of ClO_4^- anions on the two-state inclusion of **1** is summarized in Table 3. At higher ClO_4^- concentrations (>0.01 mol dm^{-3}), the higher-temperature species seems to be predominant. The application of derivative **1** to anion sensing is now in progress in our laboratories.

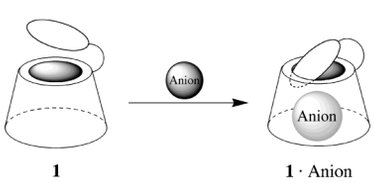

Scheme 4

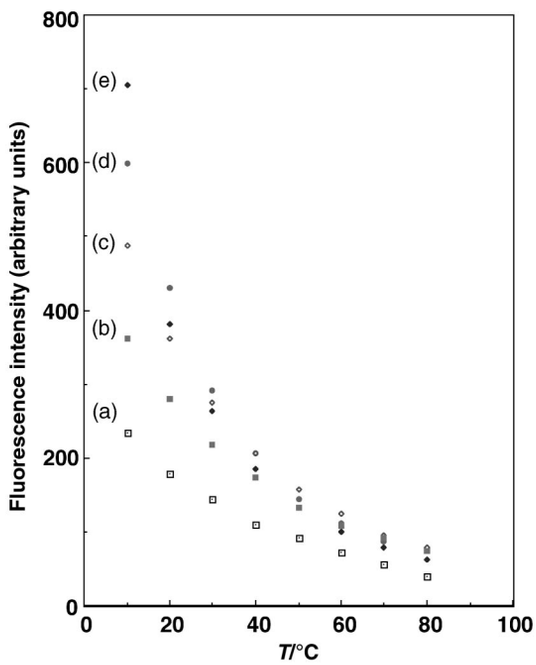

Fig. 8 Temperature-dependence of the fluorescence intensity at λ_{em}(max) for **1** at various $NaClO_4$ concentrations at pH = 6.8. [**1**] = 1.25 × 10^{-5} mol dm^{-3}. [ClO_4^-] = 0 (a), 0.01 (b), 0.1 (c), 0.5 (d), 2 (e) mol dm^{-3}.

pH dependent fluorescence of 1 and 2

Fluorescent amino-β-cyclodextrin isomers **1** and **2** have two amine sites that may be protonated. The protolytic equilibrium of the amine site linked to the fluorophore may enhance and/or quench the fluorescence of **1** and **2** owing to the chelation-enhanced fluorescence[31] or photo-induced electron-transfer (PET) mechanism.[32] Fig. 9 shows the pH dependence of the fluorescence intensity (I_f) at λ_{em}(max) of **1** and **2**. The drastic decrease in I_f of **1** upon increasing the pH from 3 to 6 could be ascribed to the deprotonation of the $-NH_2^+$ proton as shown in Scheme 5. At pH 8.5, which is closely related to the second protolytic equilibrium in Scheme 5, a much smaller decrease in I_f of **1** is observed. At pH >10, the amine sites of **1** are almost completely deprotonated and its fluorescence is consequently very low.

Since the naphthalene unit of **2** is deeply included within the CDx cavity compared with that of **1**, moderate quenching due to the first protolytic equilibrium at pH 3–6 is observed.

Table 3 Thermodynamic parameters for the inside–outside isomerization of **1** in the presence of $NaClO_4$ at 20 °C in aqueous solution

$[NaClO_4]$/M	K (20 °C)	$\Delta H°$/kcal mol^{-1}	$\Delta S°$/cal K^{-1} mol^{-1}	$\Delta G°$/kcal mol^{-1}
0	1.27	7.13	24.7	−0.14
0.01	1.16	9.11	31.3	−0.09
0.10	1.21	9.45	32.5	−0.11
0.50	1.50	11.2	39.0	−0.24
2.00	4.60	9.40	34.8	−0.89

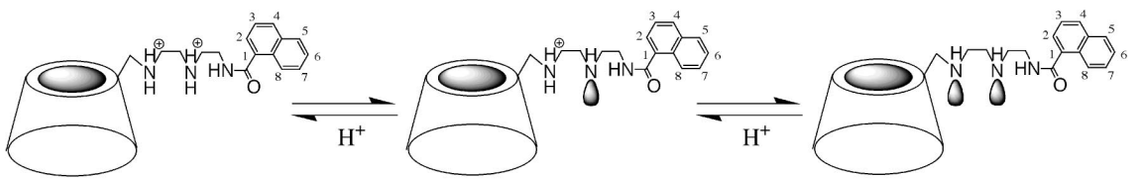

Scheme 5

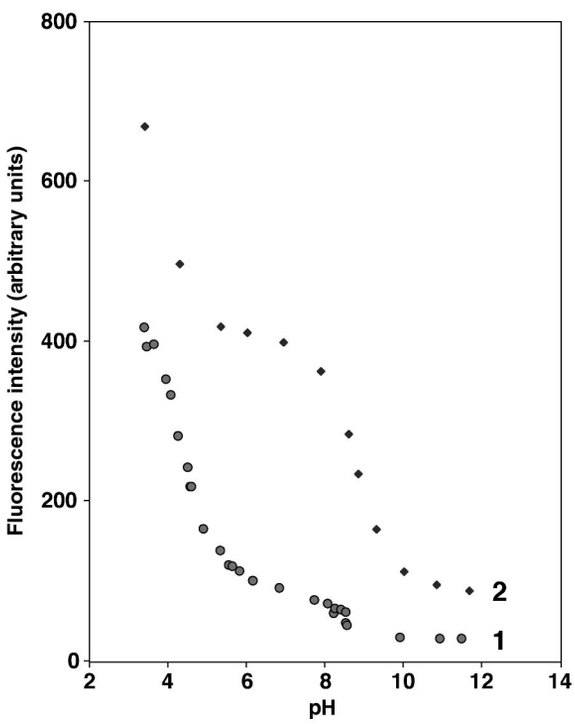

Fig. 9 Effect of pH on the fluorescence intensity at λ_{em}(max) for **1** and **2** at 25 °C. The excitation and emission bandwidth for **1** and **2** were both set at 5.0 and 3.0 nm, respectively. [**1**] = [**2**] = 1.25 × 10^{-5} mol dm^{-3}.

However, the change in I_f for **2** at pH *ca.* 8–10 is greater than that for **1**. Therefore, the pH-responsive fluorescence of **1** and **2** is controlled by two factors; the protolytic equilibria of the amine protons and to a lesser extent the pH-dependent two-state inclusion process of the naphthalene unit. ^{1}H NMR analysis at various pD values supports a reasonable correlation between the protonation–deprotonation equilibrium at the amine site and the inside–outside isomerisation of the naphthalene fluorophore.

Solvent-dependent ^{1}H NMR spectrum of 2

The driving force for inclusion of a guest into the CDx cavity is not yet clear to date,[9,10] but water inclusion in the CDx cavity and the hydrated structure around the guest molecule are crucial influencing factors in a number of host–guest systems in aqueous solution. Therefore, the inclusion process by CDx should cause a significant change both in the solvation and conformation of the naphthalene moiety and the CDx ring.

The ^{1}H NMR analysis of **2** at various temperatures revealed that the derivative **2** behaves most excellently as a NMR probe

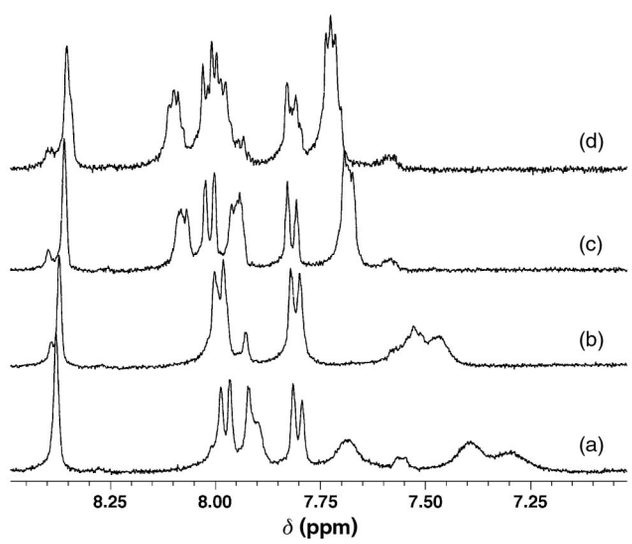

Fig. 10 ^{1}H NMR spectra of **2** at various temperatures in 10% (v/v) DMSO–D_2O mixed solvent systems (ext. ref. TMS) at 30 (a), 40 (b), 60 (c) and 70 (d) °C.

for the two-state inclusion of the appended naphthalene unit. Furthermore, this type of inclusion process may be controlled by the presence of an organic solvent such as DMSO. In fact, the two-state inclusion of **2** is fully shifted to the higher-temperature species in pure DMSO even at lower temperatures. This inclusion process is appreciably retarded by addition of 10% (v/v) DMSO into an aqueous solution of **2** as shown in Fig. 10 and is completely blocked in 50% (v/v) DMSO–water media.

Fig. 11 shows the temperature dependence of the chemical shift of the most shifted H-7 proton in the naphthalene moiety at various DMSO content. At lower concentrations of DMSO, the competitive interaction between the bulk solvent and the naphthalene moiety of **2** and/or the inclusion of a DMSO molecule leading to the formation of higher-temperature species takes place. Although the unfavourable entropic contribution ($\Delta S°_{incl} < 0$) to the Gibbs free energy term is very large, classical hydrophobic interactions ($\Delta S°_{hydrophobic} > 0$, $\Delta H°_{hydrophobic} > 0$ and $\Delta G°_{hydrophobic} < 0$), where the water is the driving force for complexation, may be less important in the inclusion process for **2**.

Conclusion

In this paper we have shown that the photophysical properties of two fluorescent amino-β-cyclodextrin isomers, **1** and **2**, bearing a naphthalene moiety linked *via* an amide bond to the CDx

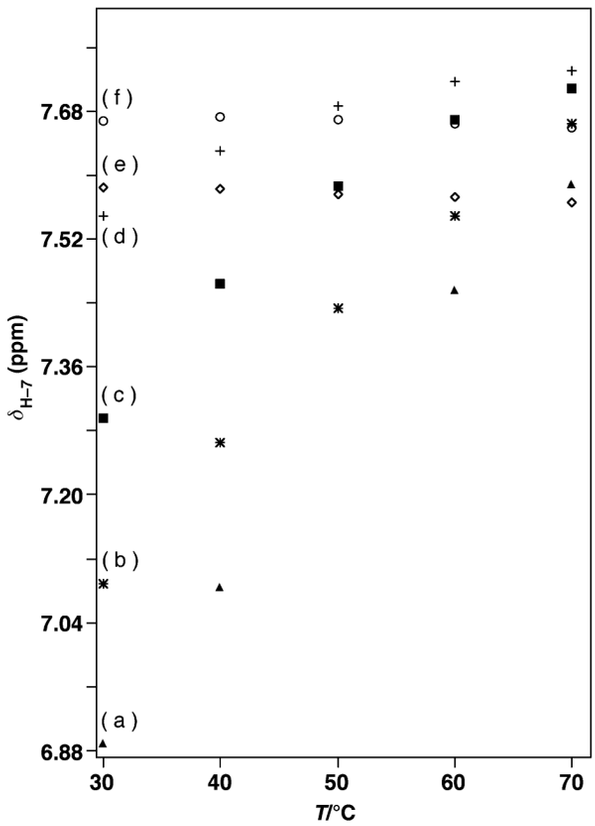

Fig. 11 DMSO (%) effect on the most temperature-dependent H-7 proton of **2** at 0 (a), 5 (b), 10 (c), 20 (d), 50 (e) and 100% (f) (v/v). Internal ref. (DSS) at 0, 5, 10 and 20% (v/v) and internal ref. (TMS) at 50 and 100%. (v/v).

ring, are greatly influenced by subtle conformational, steric and electronic differences. Quite excellent temperature and pH responses of the fluorescence of **1** and **2** in aqueous solution can be explained by a two-state inclusion model and protonation of the amino nitrogen group. The fluorescence of derivative **1** is greatly affected by the temperature change in solution, but its ^{1}H NMR signal is silent. By contrast, derivative **2** is found to be a good temperature probe by both fluorescence and ^{1}H NMR spectroscopy. It is likely that the conformational mobility of the naphthalene unit for **2** gives a more size-compatible fit in the CDx cavity. Furthermore, derivative **1** also has the possibility of acting as an anion sensor, particularly toward a hydrophobic anion such as ClO_4^- and PF_6^-. The temperature–dependent ^{1}H NMR could be controlled by the presence of an organic solvent such as DMSO. Thus, the regiospecific separation between the fluorophore and the CDx ring using the amide–amine linkage renders **1** and **2** more attractive as a fluorescence sensor.

References

1 K. E. Drexler, *Nanosystem*, Wiley-Interscience, New York, 1992.
2 J. Cao, M. C. T. Fyfe and J. F. Stoddart, *J. Org. Chem.*, 2000, **65**, 1937.
3 S. Anderson, T. D. W. Claridge and H. L. Anderson, *Angew. Chem., Int. Ed. Engl.*, 1997, **36**, 1310; S. Anderson, W. Clogg and H. L. Anderson, *Chem. Commun.*, 1998, 2379; S. Anderson, W. Clogg and H. L. Anderson, *Chem. Commun.*, 1998, 2773; J. E. H. Buston, J. R. Young and H. L. Anderson, *Chem. Commun.*, 2000, 905; C. Péan, C. Créminon, A. Wijkhuisen, J. Grassi, P. Guenot, P. Jéhan, J.-P. Dalbiez, B. Perly and F. D. Pilard, *J. Chem. Soc., Perkin Trans. 2*, 2000, 853; A. J. Baer and D. H. Macartney, *Inorg. Chem.*, 2000, **39**, 1410; D. Armspach and D. Matt, *Chem. Commun.*, 1999, 1073; S. Weidner and Z. Pilramenou, *Chem. Commun.*, 1988, 1473; G. R. Newkome, L. A. Godínez and C. N. Moorefield, *Chem. Commun.*, 1998, 1821; S. Makedonopoulou, I. M. Mavridis, K. Yannakopoulou and J. Papaioannou, *Chem. Commun.*, 1998, 2113; N. Schaschke, S. Fiori, E. Weyher, C. Escrieut, D. Fourmy, G. Müller and L. Moroder, *J. Am. Chem. Soc.*, 1998, **120**, 7030; W. Herrmann, M. Schneider and G. Wenz, *Angew. Chem., Int. Ed. Engl.*, 1997, **36**, 2511; M. Lahav, K. T. Ranjit, E. Latz and I. Willer, *Chem. Commun.*, 1997, 259; A. Harada, J. Li and M. Kamachi, *Chem. Commun.*, 1997, 1413; A. G. Meyer, C. J. Easton, S. F. Lincoln and G. W. Simpson, *Chem. Commun.*, 1997, 1517; M. D. Johnson and J. G. Bernard, *Chem. Commun.*, 1996, 185.
4 S. A. Neogodiev and J. F. Stoddart, *Chem. Rev.*, 1998, **98**, 1959.
5 D. Parker and R. Kataky, *Chem. Commun.*, 1997, 141; P. S. Bates, D. Parker and A. F. Patti, *J. Chem. Soc., Perkin Trans. 2*, 1994, 657; P. S. Bates, P. Kataky and D. Parker, *J. Chem. Soc., Perkin Trans. 2*, 1994, 669.
6 A. Seiyama, N. Yoshida and M. Fujimoto, *Chem. Lett.*, 1985, 1013.
7 A. Örstan and J. F. Wojcik, *Carbohydr. Res.*, 1988, **176**, 149.
8 A. Hersey and B. H. Robinson, *J. Chem. Soc., Faraday Trans. 1*, 1984, **80**, 2039.
9 N. Yoshida and M. Fujimoto, *J. Phys. Chem.*, 1987, **91**, 6691.
10 N. Yoshida, A. Seiyama and M. Fujimoto, *J. Phys. Chem.*, 1990, **94**, 4246.
11 N. Yoshida and K. Hayashi, *J. Chem. Soc., Perkin Trans. 2*, 1994, 1285.
12 N. Yoshida, *J. Chem. Soc., Perkin Trans. 2*, 1995, 2249.
13 N. Yoshida and Y. Fujita, *J. Phys. Chem.*, 1995, **99**, 3671.
14 N. Yoshida, H. Yamaguchi and M. Higashi, *J. Phys. Chem.*, 1998, **102**, 1523.
15 T. Kitae, T. Nakayama and K. Kano, *J. Chem. Soc., Perkin Trans. 2*, 1998, 207.
16 (*a*) H. Monzen, N. Yoshida and M. Fujimoto, *Chem. Lett.*, 1988, 1129; (*b*) N. Ito, N. Yoshida and K. Ichikawa, *J. Chem. Soc., Perkin Trans. 2*, 1996, 965.
17 A. K. Yatsimirsky and A. V. Eliseev, *J. Chem. Soc., Perkin Trans. 2*, 1991, 1769; A. V. Eleseev and H.-J. Schneider, *J. Am. Chem. Soc.*, 1994, **116**, 6081.
18 N. Yoshida, K. Harata, T. Inoue, N. Ito and K. Ichikawa, *Supramol. Chem.*, 1998, **10**, 63.
19 W. Tagaki and H. Yamamoto, *Tetrahedron Lett.*, 1991, **32**, 1297.
20 (*a*) A. Ueno, S. Minato, I. Suzuki, M. Fukushima, M. Ohkubo, T. Osa, F. Hamada and K. Murai, *Chem. Lett.*, 1990, 605; (*b*) A. Ueno, I. Suzuki and T. Osa, *Anal. Chem.*, 1990, **62**, 2461; (*c*) S. R. McAlpine and M. A. G. Garibay, *J. Am. Chem. Soc.*, 1996, **118**, 2750; (*d*) B. K. Hubbard, L. A. Beilstein, C. E. Heath and C. J. Abelt, *J. Chem. Soc., Perkin Trans. 2*, 1996, 1005; (*e*) N. Ito, N. Yoshida and K. Ichikawa, *J. Chem. Soc., Perkin Trans. 2*, 1996, 965; (*f*) R. Corradini, A. Dossena, G. Galaverna, R. Marchelly, A. Paragia and G. Sartor, *J. Org. Chem.*, 1997, **62**, 6283; (*g*) C. T. Bibeau, B. K. Hubbard and C. J. Abelt, *Chem. Commun.*, 1997, 437; (*h*) M. Narita, F. Hamada, I. Suzuki and T. Osa, *J. Chem. Soc., Perkin Trans. 2*, 1998, 2751.
21 M. Eddaoudi, H.-P. Lopez, S. F. de Lamotte, D. Ficheux, P. Prognon and A. W. Coleman, *J. Chem. Soc., Perkin Trans. 2*, 1996, 1771; S. Matsumura, S. Sakamoto, A. Ueno and H. Mihara, *Chem. Eur. J*, 2000, **6**, 1781.
22 R. A. Bissell and A. P. de Silva, *J. Chem. Soc., Chem. Commun.*, 1991, 1148; M. A. Mortellaro, W. K. Hartmann and D. G. Nocera, *Angew. Chem., Int. Ed. Engl.*, 1996, **35**, 1945; H. F. M. Nelissen, A. F. J. Schut, F. Venema, M. C. Feiters and R. J. M. Nolte, *Chem. Commun.*, 2000, 577.
23 W. Saka, Y. Yamamoto, Y. Inoue, R. Chujo, K. Takahashi and K. Hattori, *Bull. Chem. Soc. Jpn.*, 1990, **63**, 3175.
24 N. Yoshida, H. Yamaguchi, T. Iwao and M. Higashi, *J. Chem. Soc., Perkin Trans. 2*, 1999, 379.
25 K. Takahashi and K. Hattori, *Supramol. Chem.*, 1993, **2**, 305.
26 A. Ueno, F. Morikawa and T. Osa, *Tetrahedron*, 1987, 1571.
27 T. Fujimoto, Y. Sakata and T. Kaneda, *Chem. Lett.*, 2000, 764.
28 N. Poklar and G. Vesnaver, *J. Chem. Educ.*, 2000, **77**, 380; J. F. Schellman, *C. R. Trav. Carlsberg Lab., Ser. Chim.*, 1955, **29**, 230; S. Lapanje, *Physicochemical Aspects of Protein Denaturation*, Wiley-Interscience, New York, 1978, p. 187.
29 R. I. Gelb, L. M. Schwartz, B. Cardeloino, H. S. Fuhrmann, R. F. Johnson and D. A. Laufer, *J. Am. Chem. Soc.*, 1981, **103**, 1750.
30 L. A. Godfnez, B. G. S. Fiehn, S. Patel, C. M. Criss, J. D. Evanseck and A. E. Kaifer, *Supramol. Chem.*, 1996, **8**, 17.
31 *Fluorescent Chemosensors for Ion and Molecular Recognition*, ed. A. W. Czarnik, ACS Symposium Series, 1993, 538.
32 L. Fabbrizzi, M. Licchelli, P. Pallavicini, A. Perotti, A. Taglietti and D. Sacchi, *Chem. Eur. J.*, 1996, **2**, 75; A. P. de Silva, H. Q. N. Gunarathe and C. P. McCoy, *Chem. Commun.*, 1996, 2399; T. D. James, P. Linnane and S. Shinkai, *Chem. Commun.*, 1996, 281.